SOUND SOURCE CONTRIBUTIONS FOR THE PREDICITON OF VEHICLE PASS-BY NOISE

ME Braun Dept. of Aeronautical and Automotive Engineering, Loughborough University, UK
SJ Walsh Dept. of Aeronautical and Automotive Engineering, Loughborough University, UK
JL Horner Dept. of Aeronautical and Automotive Engineering, Loughborough University, UK

1. INTRODUCTION

Road traffic noise contributes to environmental noise, which can result in cardiovascular disease, sleep disturbance or annoyance for the exposed population[1]. The reduction of road traffic noise aims to increase health and life quality. Therefore, the vehicle pass-by noise emission, which is determined in a standardised test situation, was limited by legislation. First introduced in the 1970s, vehicle pass-by noise limits have been gradually reduced for all vehicle classes. However, road traffic noise was not as significantly reduced as the pass-by noise limits.

The current pass-by noise test procedure is specified in the international standard ISO 362[2]. The pass-by noise level is determined from sound pressure measurements of a number of accelerated pass-bys of the test vehicle relative to two microphones. The microphones are positioned midway in the test area on each side of the straight driving lane at a distance of 7.5 m and at a height of 1.2 m in order to measure the frequency-weighted and time-weighted sound pressure. In addition to the standardised test site, the sound absorbing properties of the test site tarmac are defined in the standard ISO 10844[3], which shall increase the reproducibility and repeatability of the test on test sites worldwide. The current test method remains unchanged in its core for many decades. In order to consider all vehicle noise sources, it is suggested to add a constant-speed pass-by test to the traditional acceleration test. Tyre/road noise would be the dominant noise source in the constant-speed test whilst the acceleration test would be dominated by powertrain-related noise sources. The final pass-by noise level would be a combination of the measured pass-by noise of both tests. In order to account for a modified test and to further reduce vehicle pass-by noise limits, new limit values as low as 68 dB(A) are proposed[5].

Prior to its market launch, a new vehicle is tested in order to certify its compliance with the standard ISO 362. During the vehicle development process, manufacturers and suppliers are required to ensure that this compliance is achieved. Hence, it is important that vehicle engineers have access to predictive tools at the design stage. In this paper a method is presented in order to predict pass-by noise contributions of vehicle noise sources using directivity measurements. Therefore, vehicle noise sources are replicated and their sound pressure radiation is quantified experimentally in directivity measurements within an anechoic chamber. The directivity sound pressure data is then combined with the inverse square law in order to predict the pass-by noise. In order to validate the pass-by noise prediction method, direct and reciprocal pass-by noise measurements are conducted with the noise source replicase within laboratory conditions.

2. THEORY FOR THE PASS-BY NOISE PREDICTION METHOD

The theory for the pass-by noise prediction of single noise sources under laboratory conditions is presented in this section. The prediction is divided into two steps. First, the noise source is quantified in the horizontal directivity measurements. Then, the directivity sound pressure is combined with the instantaneous distance between source and receiving microphone in order to predict the pass-by noise.

2.1 Directivity sound pressure measurements

For the prediction method, the noise source needs to be quantified in terms of its radiated sound pressure. Therefore, horizontal directivity measurements are carried out in which the reference point of an acoustic excitation source is positioned in the centre of a circle, which is parallel to the

ground, which is illustrated schematically in Figure 1. The radius of the circle is 1 m. Microphones are positioned on the circle in increments of 5° in order to measure the radiated sound pressure of the noise source sequentially. The microphones are on the same height as the reference point of the acoustic source. White noise is selected as the excitation signal for the vehicle noise source replicas, which are built in order to test the prediction method under laboratory conditions. The white noise signal generates a broadband response of the noise source replicas showing their characteristic acoustic properties. The vehicle noise source replicas are presented in Section 3. The radiated sound pressure is recorded in the time domain at each of the measurement positions. The data may be subject to low-pass and high-pass filtering. Then, the frequency A-weighting is applied to the data according to the guidelines of the international standard BS EN 61672-1[7]. Eventually, the time-weighted average sound pressure level (SPL) $L_{A\tau}$ is calculated according to Eq. 1 using the time constant τ = 0.125 s of the time-weighting `Fast'[2,4].

$$L_{A\tau}(t) = 10 \times \log\left(\frac{\sqrt{1/\tau \int_{-\infty}^{t} p_A^2(\xi)\exp\left(-{}^{t-\xi}/_{\tau}\right)\mathrm{d}\xi}}{p_0^2}\right) \qquad \text{Eq. 1}$$

where p_A^2 is the A-weighted instantaneous sound pressure, t is the time variable, ξ is the time integration variable, and p_0 is the reference sound pressure. In Eq. 1, the exponential function of time with the specified time constant τ is applied to weight the square of the instantaneous sound pressure. Then, the root mean square is produced, which serves as an average value, at any instant of time t. Thus, the time-varying sound pressure signal is continuously averaged, which is based on all past values of the signal. Recent sound pressure data is more weighted than older data due to the exponential function. The frequency-weighting and the time-weighting of the time history of the sound pressure data represents also a requirement in the vehicle pass-by noise test of the international standard ISO 362.

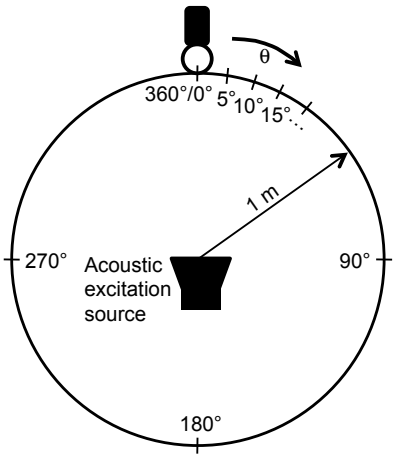

Figure 1: Schematic representation of the horizontal directivity measurements of an acoustic source.

2.2 Pass-by noise prediction

The inverse square law provides the foundation of the pass-by noise prediction method. According to the inverse square law, the squared sound pressure p_s^2 of a propagating plane sound wave in free space is inversely proportional to the squared distance r_s^2 between the source of the sound wave and the point of observation: $p_s^2 \propto 1/r_s^2$. Based on this, a relation between the sound pressure at two points of observation, which are located at different distances from the source, can be established as $p_1^2/p_2^2 = r_2^2/r_1^2$. If both distances and one of the sound pressure values are known, the other sound pressure value can be calculated using $p_1^2 = p_2^2 \times r_2^2/r_1^2$. This relation can be applied in the prediction of pass-by noise. Therefore, the sound pressure data of the directivity experiments are combined with the instantaneous distance between the noise source and the receiver as well as

the distance between the noise source and the measurement positions of the directivity experiments, which results in the prediction of a single pass-by noise value of the noise source at a specific discrete location of the noise source relative to the receiving microphone. Equation 2 is applied for the pass-by noise prediction.

$$p_r^2\left(\theta\left(t_i-\frac{r_s}{c}\right),r_s\left(t_i-\frac{r_s}{c}\right)\right)=\frac{r_{Direc}^2\times p_s^2\left(\theta\left(t_i-{}^{r_s}\!/_{c}\right)\right)}{r_s^2\left(t_i-{}^{r_s}\!/_{c}\right)} \qquad \text{Eq. 2}$$

where p_r is the predicted sound pressure at the microphone location for a particular position of the noise source on its path, p_s is the sound pressure of the source as a result of the horizontal directivity measurements, and r_{Direc} is the distance between the noise source reference point and the microphone in the directivity measurements, which is set to 1 m.

Before the pass-by noise can be predicted, a geometrical relation between the instantaneous position of the moving noise source and the static position of the receiver, which is the microphone, is to be established. This is generally based on the test layout of the ISO 362 pass-by noise test. The schematic of the test situation is illustrated in Figure 2 in which an acoustic source moves on a straight line relative to the receiving microphone. The travelled distance of the noise source is d_s and its speed is v_s. The variable t_i represents a point in time, c is the speed of sound. The instantaneous distance between the source and the microphone is r_s. The distance r_s becomes shortest when the reference point on the noise source passes the microphone, which is denoted $r_{s,pass}$. The instantaneous angle between the direction of movement of the noise source and the distance vector is θ.

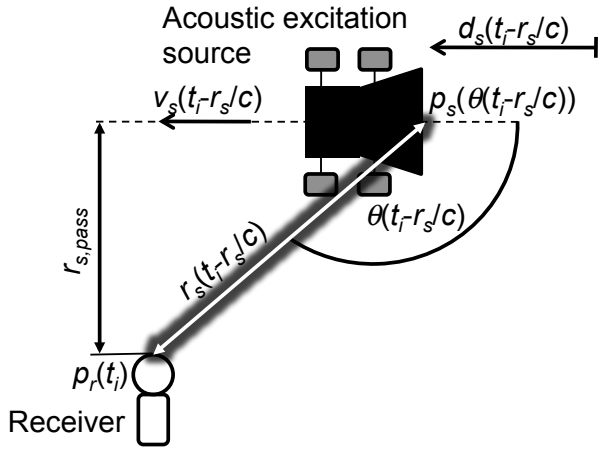

Figure 2: Schematic representation of a moving noise source on a straight line relative to a receiving pass-by noise microphone.

The travelled distance d_s of the source and its velocity v_s can be detected through various measurement devices. If the distance d_s is known, the angle θ and the distance r_s can be calculated. Since the angle θ has the same reference line and orientation in the directivity measurements and in the pass-by measurements, it can be used to select the sound pressure p_s from the measured directivity data. Linear interpolation may have to be applied in case of the angle θ lying between two adjacent directivity measurement positions. With r_{Direc} = 1 m and both the directivity sound pressure p_s and the distance r_s being available, the sound pressure p_r of the passing acoustic source can be obtained at the microphone position. Equation 2 is repeated for a number of noise source positions in order to produce a graph of discretely distributed pass-by noise prediction values against the source positions on the test track d_s. The directivity method in this form is applicable in anechoic conditions.

3. EXPERIMENTAL APPARATUS

Vehicle noise sources are replicated in order to test the pass-by noise prediction method. These are the orifice noise source (ONS) and the shell noise source (SNS), which are presented in this section. Their directivity characteristics, which are the result of the horizontal directivity experiments of Section 2, are presented as well. Finally, the application of the noise sources in the measurement of their pass-by noise, which serves as the validation data to which the predicted pass-by noise is compared, is described.

3.1 Vehicle noise source replicas

Two noise sources are replicated for the application in the prediction method. The ONS shall replicate vehicle noise sources which predominantly radiate noise from an orifice into the environment. The SNS shall replicate vehicle noise sources with thin-walled structures. Both noise sources usually lie on the outside of the vehicle and contribute well to the exterior noise radiation.

The cross-sectional view of the ONS is presented on the left-hand side in Figure11. A loudspeaker is placed in a tubular enclosure. A small plastic duct provides a waveguide from the centre of the loudspeaker diaphragm through the enclosure into the environment. The sound waves which are generated by the loudspeaker are guided through the duct in order to radiate from the duct orifice into the environment. The orifice diameter is 3 cm, which is assumed to be in the range of duct diameters of common exhaust and intake systems of passenger vehicles. Plane wave propagation is given for this duct up to a frequency of 6696 Hz[6]. The acoustic length[6] of the duct is 9 mm longer than the physical length, which indicates that the acoustic source is somewhat in front of the orifice. Thus, an end correction has to be applied to the reference point of the ONS when the distance vector r_s is calculated. The enclosure is covered by layers of sound insulation material in order to decrease the sound radiation on all sides of the ONS except the orifice.

For the experimental investigation of pass-by noise of shell structures the SNS has been built. The cross-sectional view of the SNS is illustrated on the right-hand side of Figure 3. The SNS consists of a stainless steel cylinder of the length 0.4 m and of the outer diameter of 0.16 m. There is no internal structure inside the cylinder. The cylinder is closed on one end. On the opposite end, a small opening of a diameter of 4.6 cm exists to which a duct of 3 m length is attached. On the other end of this connection duct, the previously presented ONS is attached to it in order to provide acoustic excitation for the SNS. The connection duct serves as a waveguide for the excitation sound waves. In any experiments, the ONS and the connection duct are covered with additional sound insulation material in order to minimise the effect of their sound radiation on the measured sound of the SNS.

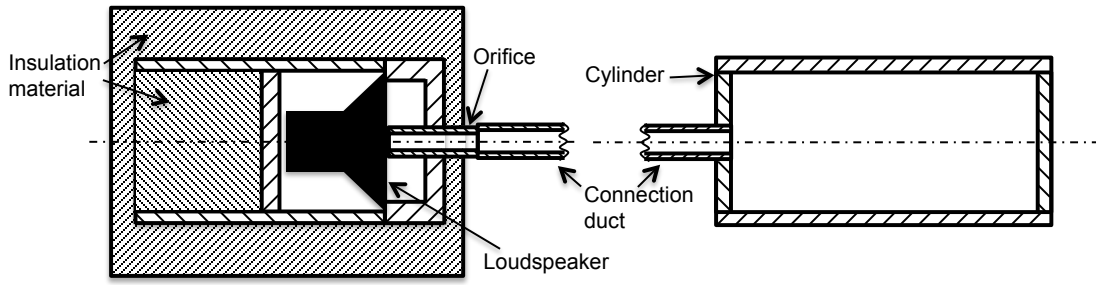

Figure 3: Cross-sectional views of the ONS on the left and the SNS on the right.

In the application of the ONS and the SNS, mass flux of air or hot exhaust gases are not reproduced. Hence, any temperature gradients within flowing exhaust gases, which alter the speed of sound and, thus, resonant frequencies of the piping system they flow through, are not considered. The ONS shall replicate the acoustic radiation characteristics of the orifice noise sources on a vehicle, like the orifice of the intake system or the exhaust system for example, for which the mixing of hot exhaust gases and ambient air is neglected. The SNS can be regarded as a simplified model of a vehicle muffler noise source.

3.2 Directivity characteristics of the noise source replicas

Experimental work is conducted according to the description in Section 2.1 in order to determine the horizontal directivity characteristics of each of the two noise sources.

The reference point of the ONS, which is used in the determination of the distance r_s between the pass-by microphone and the moving noise source, is defined as coinciding with the centre point of the orifice. This reference point is positioned in the centre of the measurement circle. The longitudinal axis of the ONS is parallel to the ground. All recordings are conducted in anechoic conditions. Figure 4 presents the measured sound pressure level L_{AT}, which is determined for the frequency range 150-6696 Hz according to Equation 1, plotted against the measurement positions. The graph of Figure 4 is regarded as the directivity characteristic of the ONS. The distribution of the SPLs is approximately symmetrical around the longitudinal axis of the ONS, which links the measurement positions at 0° and at 180°. The SPLs are much higher at the front of the ONS. Considering the region between the measurement positions of 270° and 90° as the front, the SPLs are 8-15 dB(A) higher than the levels at the rear, between 130° and 225°. The levels at the front vary within 3.2 dB(A). The levels at the rear vary within 3.9 dB(A). Between 90° and 130° as well as between 270° and 225°, the SPLs decrease rapidly by about 8 dB(A). Such level variations at the front, at the rear or at the sides of the ONS may be caused by non-uniformities in the assembly of the insulation material, as for example gaps between the layers of insulation material could decrease the attenuation capability of the assembly. The sound radiation of the loudspeaker inside the ONS is assumed to be higher towards the front and rear and to be less towards the sides. The application of insulation material at the back of the loudspeaker reduces the sound radiation towards the rear. The highest SPLs occur at the front of the ONS due to the orifice. However, the sound level which is radiated from the orifice may be less with increasing angular distance from the orifice, which can be seen at the measurement positions between 90° and 130° as well as between 270° and 225°.

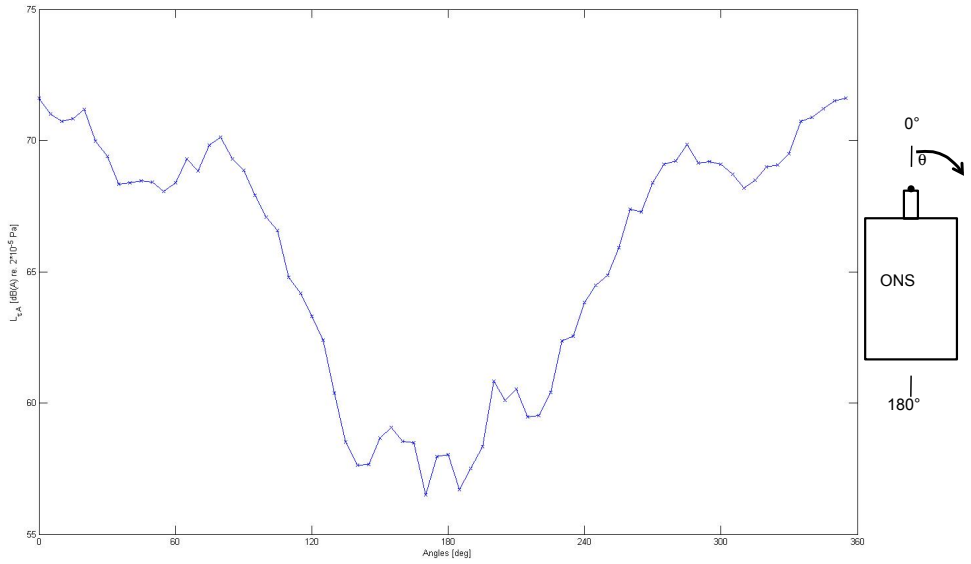

Figure 4: The exponential time-weighted SPLs with A-weighting are used to characterise the directivity of the ONS.

In case of the SNS, the reference point is defined as the geometrical centre of the cylinder. The reference point is positioned in the centre of the measurement circle. The longitudinal axis of the cylinder or the SNS, respectively, is parallel to the ground. The directivity characteristic of the SNS is presented in Figure 5 in which the measured sound pressure level L_{AT}, which is determined for a frequency range of 150-3500 Hz according to Equation 1, is plotted against the angular measurement positions. The directivity measurements cover only the angles 0°-175°, since they face the microphone during the pass-by. The SPLs at the front of the SNS are higher than the SPLs

at the rear. The trend of the SPLs appears to be decreasing the closer the measurement position is to the 180° measurement position. However, exceptions occur at approximately 70°, 90° and 150°, where the SPL reaches values which are as high or even higher than the SPL at the front of the SNS. The 70° and 150° measurement positions are approximately in the range of the edges where the cylinder meets the end plate and, thus, the edges may have an effect on the sound radiation. A dominant mode shape of the cylinder of the SNS could affect the measured SPL as well. The high SPL at the 0° measurement position could be due to the closed end of the SNS, which is a flat, thin, circular plate, which is also perpendicular to the acoustical wave propagation direction, which has its origin at the loudspeaker inside the ONS. Hence, noise may be radiated more efficiently than at the rear of the SNS, where the end plate is of an annular shape and where the connection duct interferes with the sound radiation. In addition, the weight of the cylinder acts on this end plate, which may affect the vibration properties and, thus, the noise radiation of the end plate.

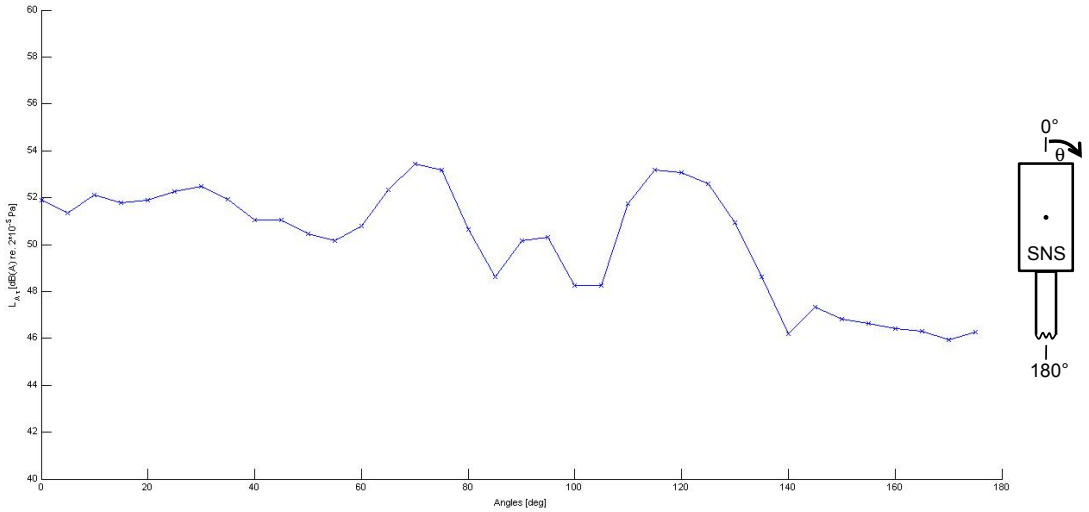

Figure 5: The exponential time-weighted SPLs with A-weighting are used to characterise the directivity of the SNS.

3.3 Experimental determination of the pass-by noise validation data

In order to validate the predicted pass-by noise levels a test rig is built on which either direct or reciprocal pass-by noise measurements are carried out with the noise sources of this work. Figure 6 illustrates the test rig schematically for the direct measurement procedure. Due to the restricted size of the laboratory facility, the length of the test rig is approximately 3 m, the test track width is 0.3 m. A winch, which is driven by an electric motor, is utilised to move a trolley on the centreline along the track. The electric motor and the winch are covered with sound insulation material in order to lower their operational noise. In the direct measurement procedure, the acoustic source is mounted on the trolley and, thus, becomes a moving noise source. The pass-by microphone is positioned midway at a distance of 0.72 m to the centreline, which results in a 53° angle towards the right and the left, thus, marking the entry and exit gates of the pass-by noise test area. This angle is equal to the ISO 362 test site. However, it has to be noted that the combination of the noise source and the experimental rig does not have an exact scaling relation to the combination of the real vehicle noise sources and the ISO 362 test track. In the reciprocal measurement setup, the noise source and the microphone swap their positions. The microphone is mounted to the trolley with its tip in line with the centreline of the test track and midway between the wheelbase of the trolley. The reference point of the acoustic source is placed at the former microphone location. Two photoelectric sensors provide the trigger signals in order to determine when the trolley enters and exits the measurement area. A RPM sensor measures the rotation of the winch against time, which can be used to estimate the velocity and the track position of the trolley during the pass-by. The validation data set is represented by the recorded pass-by noise level L_{AT} plotted against the track position of the trolley, which is shown in Section 4. Since the pass-by noise level L_{AT} is also a requirement in the standard

ISO 362, the level of reality of the laboratory scale pass-by noise experiment is increased due to the determination of L_{AT}.

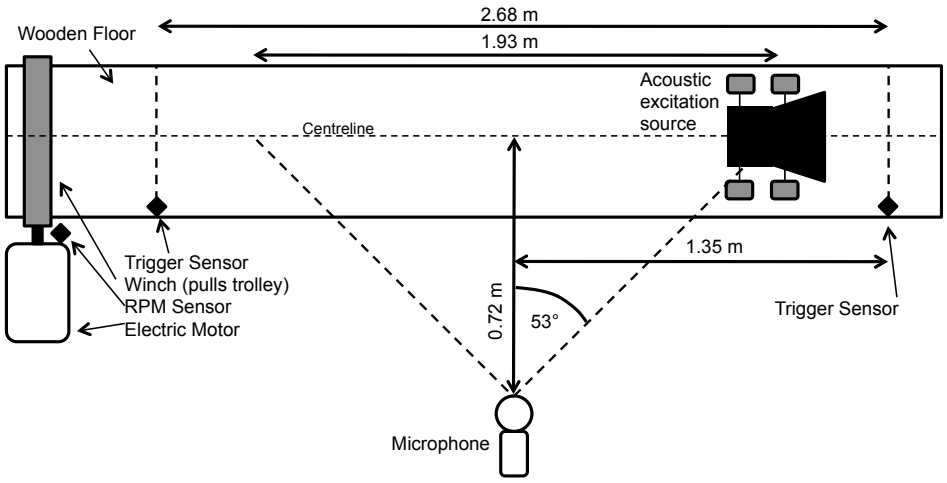

Figure 6:Schematic representation of the experimental setup for the direct measurement of the pass-by noise validation data.

4. PASS-BY NOISE PREDICTION FOR THE NOISE SOURCE REPLICAS

The prediction method of Section 2 is applied in order to predict the pass-by noise of the ONS and the SNS. The pass-by noise validation data was obtained both directly and reciprocally for the ONS and only reciprocally for the SNS due to the bulky acoustic excitation device of the SNS. In the direct procedure, the predicted and the measured pass-by noise is plotted against the coordinate of the reference point of the noise source on the test track. In the reciprocal procedure, the pass-by noise levels are plotted against the microphone position on the track.

Pass-by noise measurements and predictions are carried out for two arrangements of the ONS. First, the ONS is placed in the exhaust orifice arrangement, where the orifice points in the opposite direction of motion of the trolley. The second arrangement is the intake orifice arrangement in which the orifice points in the direction of motion of the trolley. Both arrangements are intended to simulate either an exhaust orifice or an intake orifice during the pass-by noise test. Three consecutive runs were carried out in order to record a set of validation data. The differences between the three recorded signals are generally within 0.5 dB(A) in each arrangement, hence, the repeatability is of good quality. The sudden increase of the pass-by noise level at the beginning of the recording is a consequence of the exponential time-weighted average formula for which a particular period of time must elapse before the averaged value becomes accurate. It is expected that the pass-by noise level L_{AT} becomes accurate at a distance of approximately 0.15 m.

The pass-by noise level increases steadily with distance in the exhaust orifice arrangement in Figure 7. The difference between minimum and maximum pass-by noise level is approximately 7-8 dB(A). At the beginning of the recording, the orifice points away from the microphone. The noise level rises whilst the ONS is moving, which may be related to two effects. First, since the distance between the noise source and the receiver decreases, the attenuation through distance decreases as well. Hence, the measured SPL may be increasing. Second, the relative angular positions between the noise source and the microphone alter during the pass-by, which means that the microphone is exposed to different directivity sound pressure values. In the directivity experiments, it was found that the radiated SPL varies depending upon the measurement position on the circle.
The measured pass-by noise level potentially rises since the corresponding directivity SPL increases, which is the case for the directivity measurement positions at the angles between 120° to

80°, which correspond to the altering angles during the pass-by. Then the trolley has passed the microphone position, the microphone is directly exposed to the radiated noise from the ONS and the highest directivity SPLs at the front of the orifice between ±90° affect the pass-by noise. Also, the maximum pass-by noise level of about 64 dB(A) occurs at 1.76 m. Then, the level begins to decrease slowly whilst the distance between the ONS and the microphone increases. Thus, the distance attenuation may neutralise the relatively high directivity sound pressure values at the front of the ONS. The rising and falling pass-by noise level as well as the maximum pass-by noise level appearing in the second half of the test track generally coincides with the real pass-by noise test.

The predicted pass-by noise level in Figure 7 is generally very close to the measured pass-by noise level. The highest difference between both levels is 1.3 dB(A). However, for the majority of the levels, the difference is less than 1 dB(A). This is regarded as a good result for the prediction. Both the directivity sound pressure as well as the distance between the noise source and the pass-by microphone determine the predicted pass-by noise level. Specific directivity characteristics may be recognised in the predicted pass-by noise level. The relative steady increase of the predicted pass-by noise level is related to the increase of the directivity SPL between 130° and 90°, for example. The rapid change in the gradient at 0.6 m is caused by the rapid increase in the directivity SPL between 110° and 105°. The predicted pass-by noise level between the 1.75 m mark until the end of the test track is predominantly determined by the directivity SPL between 90° and 0°, which also results in a relative good agreement with the measured pass-by noise level.

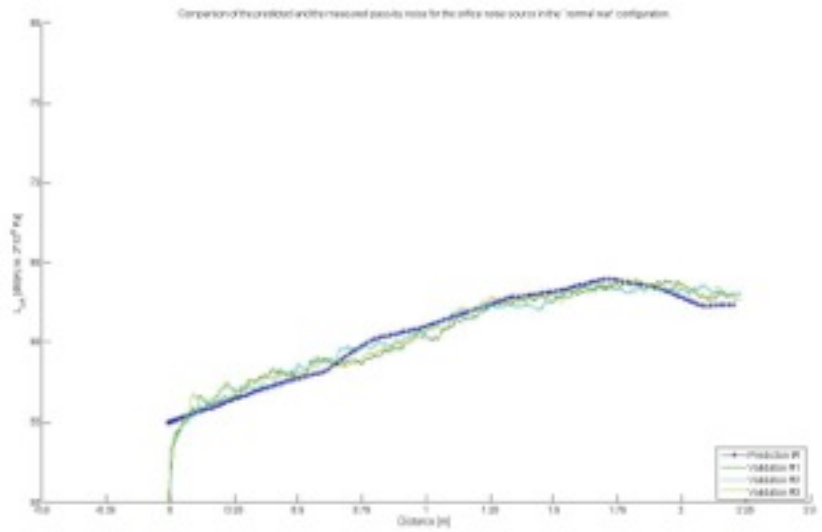

Figure 7: Comparison of the predicted and measured pass-by noise signals of the ONS in the exhaust orifice arrangement.

Figure 8 represents the predicted and measured pass-by noise levels of the intake orifice arrangement of the ONS. Compared to the pass-by noise level of the exhaust orifice arrangement, the pass-by noise level shows an opposite characteristic. After a slight increase of the pass-by noise level at the beginning of the test track, the maximum level of 64.5 dB(A) is reached at 1.15 m before the level begins to decrease until the end of the test track. The corresponding directivity SPLs at these angles are assumed to have a significant influence on the pass-by noise level. The difference between the maximum and the minimum pass-by noise level is approximately 5 dB(A). It is assumed that the characteristic rising and falling of the pass-by noise level as well as the maximum level appearing in the first half of the test track generally reflects the pass-by noise characteristics of a vehicle intake orifice noise source.

The trend of the predicted pass-by noise level in Figure 8 generally agrees well with the measured pass-by noise level. However, the predicted levels are smaller than the measured levels. In the prediction method, the directivity SPLs of the angular measurement positions of 360° to 230° are

utilised in conjunction with the calculated distance between the source and the microphone. In contrast to the measured pass-by noise level, the maximum level of the prediction, which has a value of 63.5 dB(A), appears earlier at around 0.8 m. Up to a distance of 1.35 m the difference between measurement and prediction is less than 1.5 dB(A). From approximately 1.25 m until the end of the test track the difference increases slowly but steadily. At the end of the test track the difference varies between 2.5-4 dB(A). Here, the rolling noise of the trolley may have a greater effect on the measured pass-by noise due to a decreasing directivity SPL between 270° and 230°, thus, the difference between the measured and the predicted pass-by noise is higher.

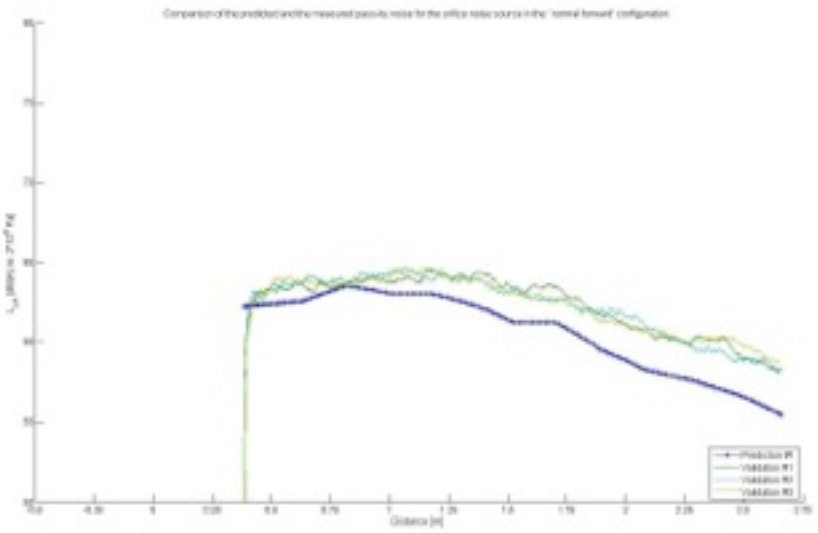

Figure 8: Comparison of the predicted and measured pass-by noise signals of the ONS in the intake orifice arrangement.

In contrast to the pass-by noise level graphs of the ONS, two maxima appear in the pass-by noise level graphs of the SNS, which are assumed to be related to the particular SNS sound radiation characteristic as illustrated in Figure 5. The pass-by noise validation data was measured reciprocally with the SNS being positioned stationary in the anechoic chamber and the microphone being attached to the moving trolley. Figure 9 represents the measured and the predicted pass-by noise levels of the SNS. The pass-by noise levels are plotted against the microphone position on the test track, which has an offset of 0.1875 m relative to the rear axle, which defines the 0 m mark for the distance axis. Again, the measured SPL L_{AT} increases rapidly at the beginning of the test track or the recording, respectively. Up to the 1 m mark the measured pass-by noise level increases by approximately 5 dB(A) to 56.5 dB(A). Then, it decreases by about 2 dB(A) until the 1.6 m mark before it rises again up to 59.5 dB(A) at the 1.9 m mark. The measured pass-by noise level decreases again towards the end of the test track reaching a value of approximately 54 dB(A). The difference between the three consecutively recorded pass-by noise levels are within 1.2-1.8 dB(A) for most of the test track length, which indicates a reasonable good repeatability of the test. However, deviations between the measured pass-by noise levels increase between the 1.7 m and the 2 m marks with different values for each recording. The highest deviation is 2.2 dB(A) at 1.9 m. It appears that a random measurement error may be the cause for these deviations. Whilst the second and the third recording represent the lowest and the highest pass-by noise levels, the first recording shows values which are almost equal to the second recording in the first half. In the second half, the values of the first recording rise and become almost equal to the values of the third recording.

The predicted pass-by noise level differs from the measured level. However, the trend of the predicted and the measured pass-by noise levels are similar up to the 1.25 m mark, where the distance between the microphone and the SNS decreases and the pass-by noise level generally increases. The deviation between prediction and measurement is initially about 3 dB(A), but it is

reduced slowly afterwards and becomes lowest with a deviation of 1.2 dB(A) at the maximum pass-by noise level at 1.1 m, which indicates a good result produced with the prediction method. Up to the 1.5 m mark, the predicted pass-by noise level decreases first, then it increases to a local maximum before it decreases again. The comparison with the validation data is rather poor, as it shows only a decreasing trend and not a local maximum. The deviations between prediction and measurement is in the range of up to 4 dB(A). From the 1.5 m mark, both the predicted and the measured data show rising levels with small deviations of less than 1.5 dB(A) at around the 1.7 m mark, which is considered as a reasonable result. The maxima at 70°, 95° and 115° in the directivity SPL of the SNS are reflected in the local maxima at 1.1 m, 1.4 m and 1.7 m of the predicted pass-by noise level. The trend of the falling pass-by noise level between 1.7-2.2 m is matched well only between the 2-2.2 m marks despite deviations between 6-9 dB(A). From the 2.3 m mark until the end of the test track, the predicted levels are approximately constant, which is matched by the first and second recording of the validation data. However, deviations between prediction and validation data become high up to 9.6 dB(A). Despite the coverage with additional sound insulation material, such deviations might be caused from the sound radiation of the connection duct and the ONS or even the operational noise of the winch system of the pass-by noise test rig. This could be detected with the microphone on the trolley when it moves towards the end of the test track since the distance between the microphone and the connection duct as well as the ONS becomes closest there, whilst the sound radiation from the SNS may be slightly attenuated due to the increasing distance. The values of the measured as well as the predicted pass-by noise levels are generally low, which is assumed to be related to the acoustic excitation apparatus despite being set to operate at the maximum possible power output.

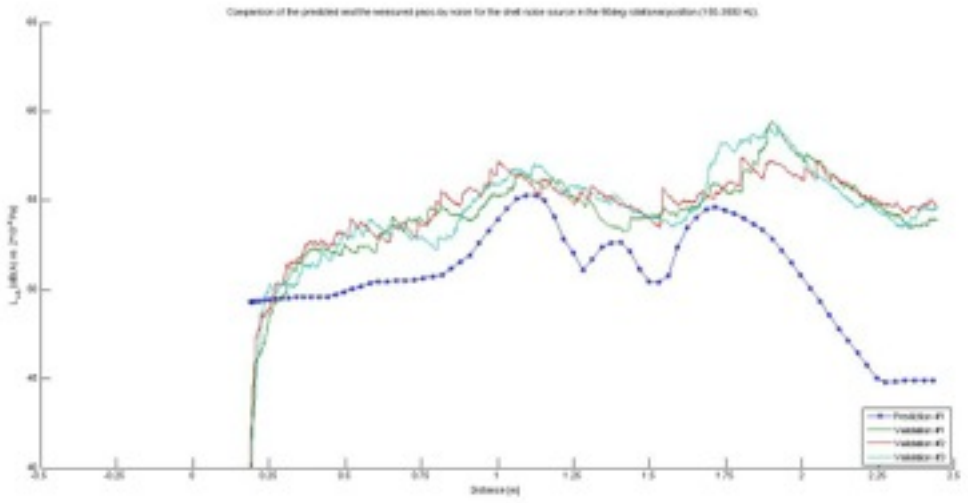

Figure 9: Comparison of the predicted and measured pass-by noise signals of the SNS.

5. SUMMARY AND CONCLUSION

A pass-by noise prediction method for single noise sources has been presented. The prediction method combines the instantaneous distance between the noise source and the microphone in the pass-by noise test with the directivity sound pressure, which is obtained individually for every noise source. In order to test the method two vehicle noise sources are replicated, the orifice noise source (ONS) and the shell noise source (SNS). Pass-by noise validation data is measured utilising the vehicle noise source replicas and a laboratory scale pass-by noise test rig.

The pass-by noise prediction of the ONS in the exhaust orifice arrangement achieves very good results. In case of the ONS in the intake orifice arrangement, the deviations between the predicted and the measured pass-by noise are slightly higher than in the previous arrangement. However, the result is regarded as good. In case of the SNS, the prediction results show the highest deviations of

the three pass-by noise configurations. However, the results are reasonably good for both maximum SPLs as well as the trend of the predicted pass-by noise level which matches the measured one for most regions of the test track. The prediction method depends on the determination of the distance between the noise source and the microphone during the pass-by as well as on the directivity sound pressure measurements. The linear interpolation of directivity sound pressure between adjacent measurement positions is used for the prediction and, thus, may cause an error, since the directivity sound pressure may not be entirely of a linear characteristic. In addition, the measurement of the pass-by noise validation data has to be carried out with caution in order to avoid any recording of background noise, which may lead to misinterpretation of results. Overall, the applicability of the prediction method for the estimation of the pass-by noise contribution of the ONS has been shown. The effort for its execution is relatively low. Such pass-by noise prediction results could be used to identify high contribution to the pass-by noise from every vehicle noise source and, thus, be able to estimate whether the successful completion of the vehicle pass-by noise test is at risk.

6. REFERENCES

1. L. Fritschi, et al., Burden of disease from environmental noise – Quantification of healthy life years lost in Europe, World Health Organization Regional Office for Europe. Copenhagen (2011).
2. British Standard ISO 362, Acoustics – Measurement of noise emitted by accelerating road vehicles – Engineering method. London (1998).
3. British Standard ISO 10844, Acoustics – Specification of test tracks for measuring noise emitted by road vehicles and their tyres. London (2011).
4. British Standard ISO 362-1, Measurement of noise emitted by accelerating road vehicles – Engineering method – Part 1: M and N categories. London (2007).
5. F. De Roo, VENOLIVA – Vehicle Noise Limit Values – Comparison of two noise emission test methods – Final Report. Delft (March 2011).
6. M. L. Munjal. Acoustics of ducts and mufflers (with application to exhaust and ventilation design), John Wiley & Sons, New York, USA (1987).
7. British Standards Institution. Electroacoustics - Sound level meters - Part 1: Specifications, BS EN 61672-1:2003, London (2003)